THE JOURNAL OF PHYSICAL CHEMISTRY LETTERS
A JOURNAL OF THE AMERICAN CHEMICAL SOCIETY

pubs.acs.org/JPCL Letter

Synthesis of Weaire–Phelan Barium Polyhydride

Miriam Peña-Alvarez,* Jack Binns, Miguel Martinez-Canales, Bartomeu Monserrat, Graeme J. Ackland, Philip Dalladay-Simpson, Ross T. Howie, Chris J. Pickard, and Eugene Gregoryanz*

HPSTR 1193-2021

Cite This: J. Phys. Chem. Lett. 2021, 12, 4910–4916 Read Online

ACCESS | Metrics & More | Article Recommendations | Supporting Information

ABSTRACT: By combining pressures up to 50 GPa and temperatures of 1200 K, we synthesize the novel barium hydride, Ba_8H_{46}, stable down to 27 GPa. We use Raman spectroscopy, X-ray diffraction, and first-principles calculations to determine that this compound adopts a highly symmetric $Pm\bar{3}n$ structure with an unusual $5\frac{3}{4}$:1 hydrogen-to-barium ratio. This singular stoichiometry corresponds to the well-defined type-I clathrate geometry. This clathrate consists of a Weaire–Phelan hydrogen structure with the barium atoms forming a topologically close-packed phase. In particular, the structure is formed by H_{20} and H_{24} clathrate cages showing substantially weakened H–H interactions. Density functional theory (DFT) demonstrates that cubic $Pm\bar{3}n$ Ba_8H_{46} requires dynamical effects to stabilize the H_{20} and H_{24} clathrate cages.

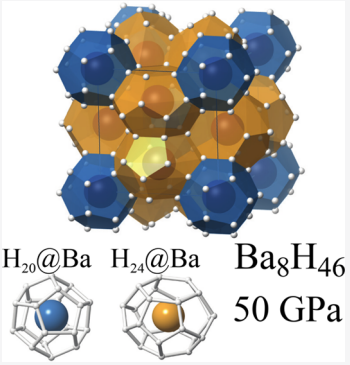

Strongly electropositive elements can readily donate electrons ($E \rightarrow E^+ + e^-$) into antibonding orbitals of molecular hydrogen (H_2), weakening the H–H covalent bond. It has been proposed that the combination of electropositive elements and high pressures should promote the dissociation of molecular H_2 at lower pressures than in pure H_2, often referred to as chemical precompression.[1−9] Despite being proposed in 2004,[1] it is only in recent years that an abundance of new hydrogen-bearing systems have been uncovered, exhibiting superconductivity with high critical temperatures, albeit at ultrahigh pressures.[10−12]

The alkaline and alkaline-earth metals are exemplary electropositive elements and can readily donate electrons to occupy the antibonding state (σ^*) of molecular hydrogen. Early structural searches in the calcium hydrogen system (Ca–H) predicted the formation of the hexahydride CaH_6 (space group $I4\bar{3}m$) based on a body-centered cubic (bcc) Ca lattice. Within this system the Ca atoms are enclathrated by hydrogen cages interlinked, forming H_4 units as building blocks of a three-dimensional sodalite-like framework. The hydrogen cages would present H–H distances significantly longer than those of molecular hydrogen.[3,13,14] Subsequent theoretical works predicted similar structural motifs in the rare-earth metal hydrides YH_6 (stable above 300 GPa) and LaH_{10} (stable above 200 GPa).[15,16] From the theoretical predictions, hydrogen clathrate cages are motifs promoting superconducting properties.[17,18]

Clathrate cages appear in many diverse materials such as ices[19,20] or silicon-based structures.[21−23] In particular, hydrogen clathrates became relevant with the synthesis of LaH_{10} with H_{32} cages,[24,25] and LaH_{10} is claimed to possess a superconducting critical temperature (T_c) between 250 and 260 K at around 200 GPa.[10,11,24] However, despite laying claim to the discovery of high-temperature superconductivity, this study along with other recent discoveries of other hydrogen-bearing systems with high T_c[12] suffer from another thermodynamic parameter, namely, pressure. These new hydrogen-bearing materials require pressures in excess of 150 GPa for synthesis, a significant challenge to becoming technologically relevant. Therefore, to achieve the ultimate goal of applicable room pressures and temperatures, one needs first to find a pathway to nonmolecular hydrides at conditions closer to the ambient.

Electropositive elements at high pressure have been predicted to form highly symmetric hydrogen clathrates.[1−9,26] Some alkaline and alkaline-earth elements form type-I clathrates structures with silicon (Si) with low-temperature superconducting properties.[22,23] However, these clathrates have not yet been seen in its hydrogen analogue, neither experimentally nor theoretically, so the effect of hydrogen substitution is yet to be explored.[5,7,27] The pressures at which the alkaline-earth polyhydrides stabilize correlate with their ionization potentials.[8] Thus, electropositive elements are ideal to search for clathrate-based structures. Beryllium (Be) and H_2 form $Be_4H_8(H_2)_2$ crystallizing in a $P6_3/mmc$ structure which consists of corner-sharing BeH_4 tetrahedra and H_2 molecules

Received: March 14, 2021
Accepted: April 16, 2021
Published: May 19, 2021

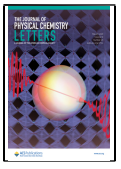

https://doi.org/10.1021/acs.jpclett.1c00826
J. Phys. Chem. Lett. 2021, 12, 4910–4916

occupying an interstitial site.[28] Magnesium (Mg), less electropositive than Ca, was predicted to form MgH_6 with the same sodalite-type structure as CaH_6 at higher pressures of 300 GPa.[29] The heavier alkaline-earth hydrides form with strontium (Sr) and barium (Ba), i.e., SrH_6 and BaH_6, at 150 and 50 GPa, respectively.[5,6] However, the most favored structures for both did not resemble any clathrate-like structure.[5,6] In fact, BaH_{12} was recently synthesized at 90 GPa, whose structure is characterized by H_2, H_3^- units, and H_{12} chains with a T_c of 8−20 K.[5,27]

We explore the formation of highly symmetric hydrogen cages with barium atoms as the host, combining X-ray diffraction (XRD), Raman spectroscopy, density functional theory (DFT), and *ab initio* molecular dynamics. Heating Ba or BaH_2 in hydrogen to 1200 K at 50 GPa leads to the formation of a novel compound. X-ray diffraction patterns indicate that the product adopts a highly symmetric $Pm\bar{3}n$ structure, which was stable on decompression to 27 GPa. Our approach shows its structure to be a type-I hydrogen clathrate with a Ba_8H_{46} composition. Theoretical calculations reveal that the Ba_8H_{46} hydrogen cage structure represents a Weaire−Phelan clathrate allowing the strange allocation of $5\frac{3}{4}$ hydrogen atoms per barium.[30] This unexplored configuration is a structure type formed by hydrogen polyhedral cages of 14 and 12 faces with H−H distances varying between 0.86 and 1.4 Å. The symmetric $Pm\bar{3}n$ Ba_8H_{46} structure is metallic, but it is dynamically unstable. *Ab initio* molecular dynamics demonstrate its mechanical stability at room temperature and beyond.

As the starting materials we use pure Ba (99%) or BaH_2 (99.5%) loaded together with research grade H_2 at 0.2 GPa.[31,32] Independent of the staring material we observe BaH_2 and H_2 after loading at below 1 GPa as seen by Raman spectroscopy and/or X-ray diffraction (Figures 1 and 2). Our results on BaH_2 agree with those previously reported; at ambient conditions BaH_2 crystallizes in the contunnite structure (*Pnma*), undergoing a transition to the hexagonal Ni_2In BaH_2−II ($P6_3/mmc$), between 1.6 and 2.3 GPa,[34,35] adopting a metallic AlB_2-type structure, BaH_2−III, at 40−50 GPa.[34,36] We did thorough searches to preclude contamination, Figures S1−S3. In Figure 1 between 0.6 and 33 GPa, the spectra show pure H_2 and BaH_2. H_2 modes consist of the low-frequency rotational modes and E_{2g} phonon[32,33] and H−H stretching at around 4200 cm^{-1}.[31] BaH_2 features are assigned for BaH_2−I at 0.6 GPa with Ba−Ba stretching modes at 90 cm^{-1} and Ba−H modes between 500 and 800 cm^{-1}[34−36] and for BaH_2 between 7 and 35 GPa.[34−36] When pressure is increased further, a novel phase referred to as BaH_x appears. Even though the changes in Raman spectra are quite significant (Figure 1), the X-ray pattern remains the same (Figure 2(a)). This will be described in a separate publication.[37]

BaH_2 in H_2 was further compressed to 45 GPa and laser heated using a YAG laser (λ = 1064 nm), reaching temperatures of 1200 K and leading to dramatic changes in the observed Raman and diffraction patterns (Figures 1 and 2). All observed peaks could be uniquely indexed to a mixture of BaH_2 and a second phase with a primitive cubic unit cell a = 6.8476(4) Å; systematic absence analysis suggested space group $Pm\bar{3}n$. The thermal energy provided by heating not only drives the synthesis of a new phase but also leads to the completion of the sluggish transition from BaH_2−II to BaH_2−III. As in the case of BaH_x, the amount of free hydrogen in the sample chamber appears to be reduced (Figure 1), but more

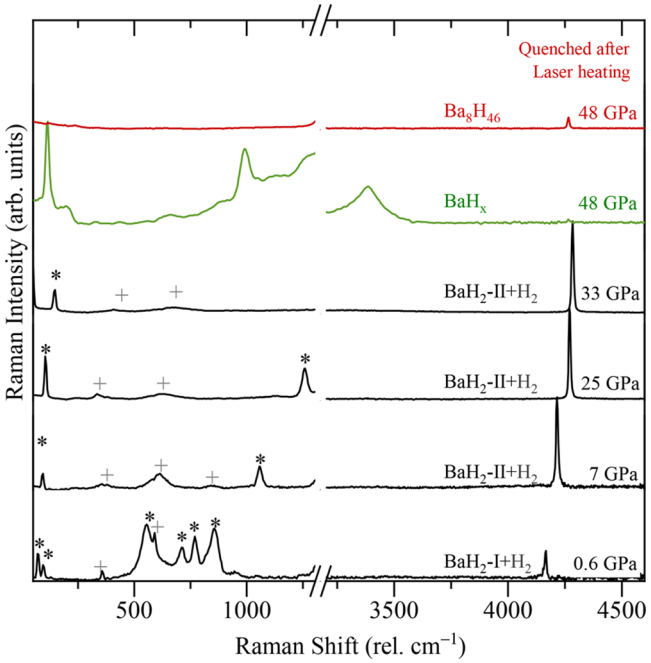

Figure 1. Raman spectra on compression of BaH_2 and H_2. Green spectra are of a product formed just by compression of BaH_2 in H_2 at room temperature, assigned as BaH_x as the X-ray diffraction does not allow its assignment.[37] The red spectrum corresponds to Ba_8H_{46} formed after laser heating at around 1200 K. The H_2 rotons are marked with a gray plus (+) symbol, while BaH_2 excitations[35] are marked with an asterisk (*) symbol. The spectral region between 1300 and 3250 cm^{-1} for the first- and second-order Raman spectra of diamond are cut for clarity, and the whole spectra can be seen in Figure S3.

interestingly, the novel phase does not have any detectable Raman activity, a common feature among the metallic hydrides described to date.[10,11,27] The were 10 repeated experimental runs, using Ba and BaH_2 with H_2 as precursors, and the same structural changes were detected. The samples after laser heating were thoroughly mapped by Raman and XRD analyses, and no sign of presence of any other structure or hydrides could be detected.

Structure solution of the novel phase by direct methods[39] reveals two Ba sites, 2*a* and 6*d*. Two-phase Rietveld refinement of the quenched diffraction patterns using only the Ba positions shows excellent agreement with the data, confirming the underlying Ba substructure (Figure 2(b, c)). The structure of this phase differs significantly from all postulated phases for barium polyhydrides including BaH_6 (*Fddd*, *P*4/*mmm*, and *Imm*2), BaH_{10} (*C*2*c*, *Cm*, and *Cmmm*), and BaH_{12} (*Cmc*2_1, $Fm\bar{3}m$, and *P*2/*m*).[5,27] The novel hydride has no detectable Raman activity (Figure 1 and Figure S3). These observations are analogous to the changes observed during the formation of the lanthanide superhydrides[10] or BaH_{12}.[27] The low X-ray scattering power of hydrogen precludes direct determination of atomic positions and exact stoichiometry of this novel compound. Examination of the unit-cell volumes with changing pressure implies a Ba/H ratio approximating 1:6, assuming ideal mixing of the elements (Figure 3(a)). This experimental results are the basis for the structure determination.

We used DFT-based structure predictions, AIRSS,[40,41] and CASTEP[42] to fully determine the experimentally observed

https://doi.org/10.1021/acs.jpclett.1c00826
J. Phys. Chem. Lett. 2021, 12, 4910−4916

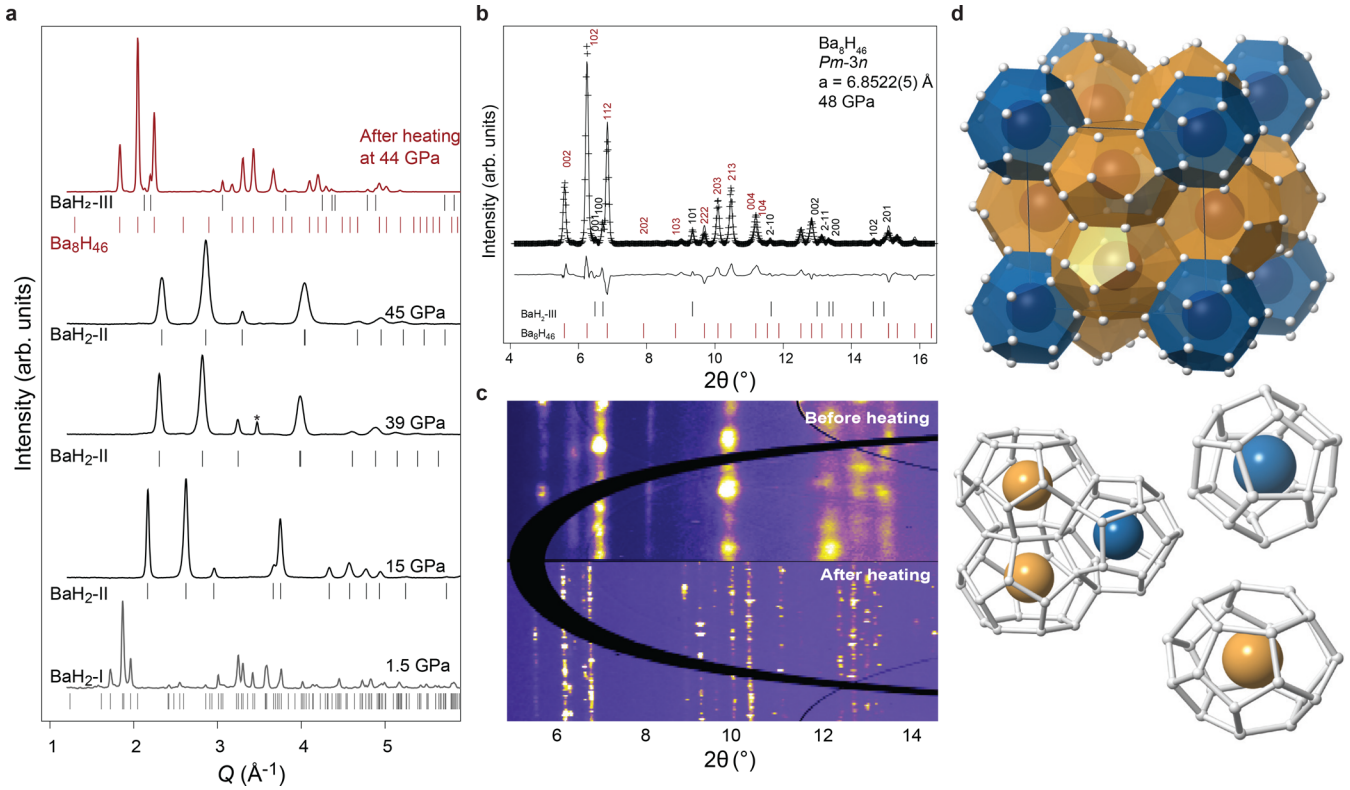

Figure 2. (a) High-pressure X-ray diffraction patterns demonstrating the synthesis of Ba_8H_{46} by laser heating mixtures of BaH_2 and H_2 above 45 GPa. Tick marks indicate Bragg peaks from the labeled phases. Peaks marked with asterisks are from the Au pressure marker.[38] Data are shown in q for consistency between compression and subsequent laser heating runs. (b) Representative Rietveld refinement of cubic Ba_8H_{46} at 48 GPa (λ = 0.3344 Å). The difference between observed and calculated profiles is shown above the tick marks. wR_p = 3.20% wR_{all,BaH_2} = 11.36% and $wR_{all,Ba_8H_{46}}$ = 13.10%. (c) 2D XRD image plates before and after laser heating (λ = 0.3344 Å). (d) $Pm\bar{3}n$ Ba_8H_{46} crystal structures, highlighting the clathrate cages (top) and the Ba-encapsulating polyhedra (bottom). BaH_{20} dodecahedra and BaH_{24} tetrakaidecahedra are shown in blue and yellow, respectively.

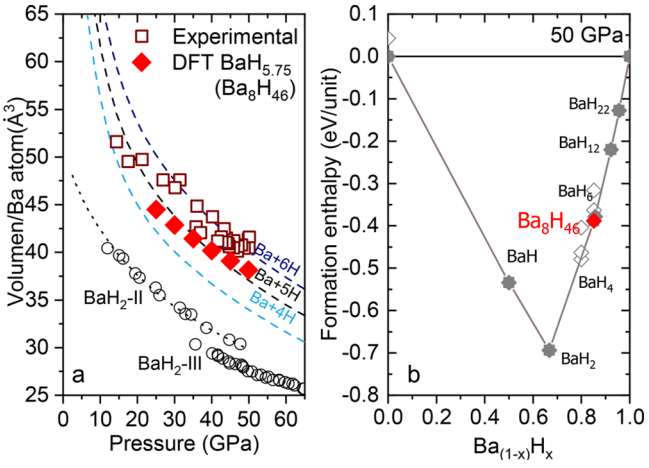

Figure 3. (a) Volume per Ba atom for various Ba−H compounds. Open symbols correspond to the experimental results and filled symbols to the DFT-calculated ones for Ba_8H_{46}. (b) Convex hull construction for Ba + $(1/2)(H_2)_{n-2}$ phases relative to Ba and 1/2 H_2, at 50 GPa. Empty (filled) symbols denote metastable (stable) compositions.

structure, based on the approximate observed hydrogen content and well-identified Ba positions. Initial searches were guided by the experimental volumes on suspected $BaH_{3/4/6}$ stoichiometries, complemented with alternative compositions to determine the energy landscape. Identifying the Ba sublattice as a clathrate showed Ba_8H_{46} to be a competitive composition. The stoichiometry was confirmed by performing compatible high-symmetry searches with different hydrogen content, with Ba_8H_n (n = 41−46) and other clathrates, with only n = 46 being competitive.

These high symmetry searches confirm the $Pm\bar{3}n$ space group symmetry, with hydrogen occupying the 6*c*, 16*i*, and 24*k* Wyckoff sites, corresponding to a stoichiometry of Ba_8H_{46}. As shown in Figure 3(b), Ba_8H_{46} lies on the convex hull at 50 GPa. This structure is constructed by the packing of two distinct kinds of atomic hydrogen clathrate cages around each Ba-atom site (Figure 2(d)), i.e., a face-centered cubic array of BaH_{20} dodecahedra adjacent to BaH_{24} tetrakaidecahedra. This structure is a form of the Weaire−Phelan network, a solution to the Kelvin problem of efficient cellular packing, the lowest energy configuration of packed bubbles of equal size.[43] This structural type has been observed in type-I clathrate structures and alkali metal silicides which share the same A_8B_{46} stoichiometry (e.g., Ba_8Si_{46} and Na_8Si_{46}).[21−23,44,45] Interestingly, Ba_8Si_{46} is superconducting with a critical temperature of 4−9 K.[46,47] The study of the superconducting properties is out of the scope of this work.

Although Ba_8H_{46} is the first recognized hydride adopting this type-I structure, this stoichiometry was also reported as one of a number of mixed phases in europium hydrides above 90 GPa. However, the novelty of the structural type was not emphasised.[48] Thus, it is possible that this Weaire−Phelan structural motif could be more ubiquitous in other systems.

https://doi.org/10.1021/acs.jpclett.1c00826
J. Phys. Chem. Lett. 2021, 12, 4910−4916

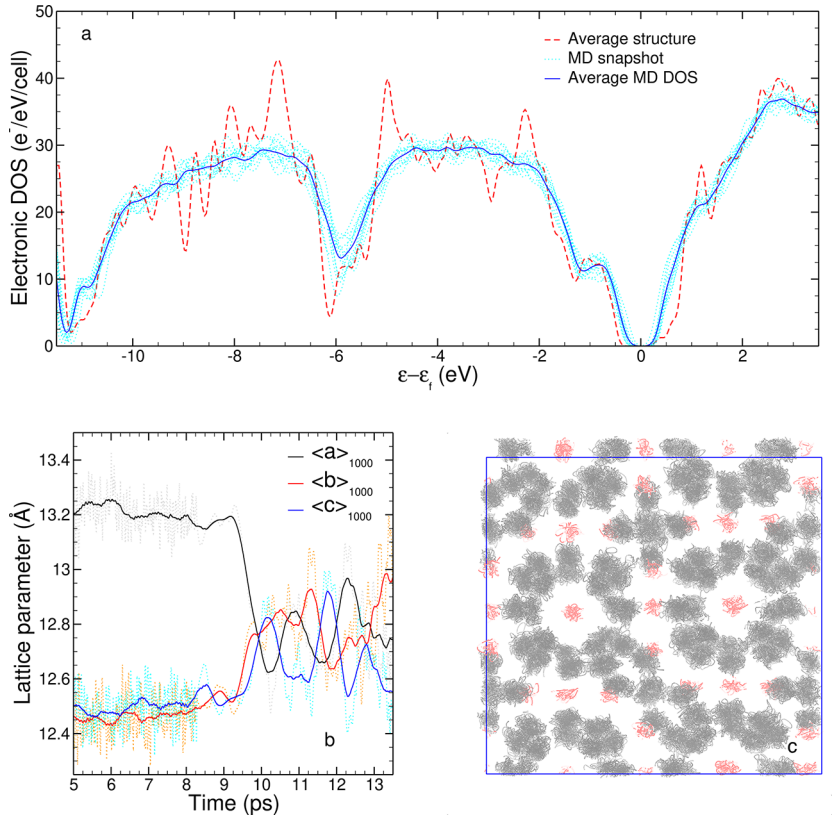

Figure 4. (a) Electronic density of states of the Ba_8H_{46} $Pm\bar{3}n$, using BOMD snapshots at 50 GPa and the time-averaged structure. (b) Evolution of the lattice parameters of Ba_8H_{46} along the 100 GPa simulation. The dotted black, orange, and cyan lines represent *a*, *b*, and *c*, respectively. The continuous black, red, and blue lines represent the 1000-step running average of *a*, *b*, and *c*, respectively. Temperature is increased from 300 to 600 K at 8.4 ps. About 1 ps after the temperature increase, there is a clear transition from the initial $P4_2/mnm$ structure. This is a symmetrization toward the $Pm\bar{3}n$ structure. (c) Trajectory of barium (pink) and hydrogen (gray) atoms within the MD simulation between 10 and 13.5 ps.

The unusual 1:$5\frac{3}{4}$ stoichiometry is readily understood as the maximum possible amount of interstitial atomic hydrogen in any Ba lattice. We assume that the Ba lattice is fixed and that solubility is driven by the physical densification of the mixture under pressure (the *PV* term in the free energy). However, maximizing the hydrogen content packing competes with chemical bonding, which induces a Jahn−Teller distortion on the cubic structure. The formal definition involves partitioning space into polyhedra with a Ba on each vertex. Each polyhedron forms an interstitial site. Ba_8H_{46} means that hydrogen atoms form Voronoi polyhedra around each barium atom, where all the polyhedra are tetrahedrons and each contains precisely one hydrogen. These Voronoi polyhedra are the bubbles in the Weaire−Phelan foam. For metals under ambient conditions, small amounts of dissolved hydrogen are always located in such interstitial sites. So, $5\frac{3}{4}$ is a special value, representing the upper limit for the amount of hydrogen which can be absorbed in this particular way. Compounds with higher than 1:$5\frac{3}{4}$ hydrogen content cannot have every hydrogen in its own 3D "cage" of barium atom.

Calculated distances between hydrogens from the static $Pm\bar{3}n$ structure at 25 GPa range from 0.86 to 1.8 Å (Figure S5(d)), becoming more homogeneous with pressure (see Figure S5(e)). Comparing the Ba_8H_{46} shortest H−H first-neighbors' distances with those of molecular H_2, in the Weaire−Phelan barium polyhydride these are elongated between 11−15% in the pressure range between 25 and 50 GPa. LiH_6, not predicted to form a clathrate-type structure but to be metallic at 100 GPa, had H−H distances around 1.45 Å,[2] while in CaH_6 these were 1.24 Å at 150 GPa[49] and in LaH_{10} around 1.19 Å at 150 GPa (see Figure S5(e)).[24] Therefore, Ba_8H_{46} exhibits H−H distances at 50 GPa comparable with those other polyhydrides at 150 GPa.

At the classical harmonic limit, the lowest enthalpy $Pm\bar{3}n$ Ba_8H_{46} is not stable, undergoing symmetry-breaking distortions (Figure S6); the $Pm\bar{3}n$ structure distorts a $\sqrt{2} \times \sqrt{2} \times 1$ supercell (equivalent $c/a = 1.06$) to a tetragonal $P4_2/mnm$ structure and also a 3° monoclinic distortion to *Pc* (Figures S4, S6, and S7). These distortions are not compatible with the observed X-ray diffraction pattern which clearly fits into the $Pm\bar{3}n$ structure. Structure stability must be strongly influenced by hydrogen fluctuations, as in CaH_6 and LaH_{10}.[49,50]

Via Born−Oppenheimer molecular dynamics (BOMD), we explore whether large hydrogen motion stabilizes the high symmetry Ba_8H_{46} $Pm\bar{3}n$. Our 432-atom BOMD simulations take the tetragonal Ba_8H_{46} structure ($P4_2/mnm$) at 100 GPa as a starting point. This was stabilized for 1 ps at 300 K in the NVT ensemble, then changed to NPT, and allowed for cell shape distortions. Monitoring the angles for the next 7.4 ps showed the stability of the tetragonal candidate; the average monoclinic distortion was ~0.5°, which is 6 times smaller than the static value. We then raised the temperature to 600 K to mimic increased hydrogen mobility and dynamics.[51]

https://doi.org/10.1021/acs.jpclett.1c00826
J. Phys. Chem. Lett. 2021, 12, 4910−4916

After 1 ps, the long axis collapses by 4% while the short axes expand, and they start fluctuating at about the same values (Figure 4(b), see Figure S8 for angles). This symmetrization is not a consequence of melting or superionic diffusion of the hydrogen lattice; despite the higher temperature, each hydrogen atom remains within its tetrahedral site, its average position being at the center and the larger fluctuations in the mean square displacement (MSD) (Figure S9). Figure 4(c) shows the Ba and hydrogen trajectory within the MD calculations between 10 and 13.5 ps. The BOMD averaged symmetry (Figure 4(b)) is fully consistent with the experiment. Figure 4(a) shows the averaged electronic density of states (DOS) at a series of random snapshots after the cubic transition. This has been compared with the DOS of the average structure, where the positions and lattice parameters were averaged over the last 4 ps of the MD. The average MD DOS is semiconducting/semimetallic, with a gap of about 0.2 eV, consistent with the observed metallic luster.

For Ba_8H_{46}, valence bond theory implies a composition of $(BaH_2)_8(H_2)_{15}$. Since each hydrogen atom is located in its own tetrahedral cage, formation of fully molecular hydrogen is strongly inhibited by the putative "bond" passing through a triangle of Ba atoms. Analysis of the species-decomposed radial distribution function (RDF) shows that approximately 15 H−H bonds (Figure S10) lie in the first peak with some ambiguity because RDF does not decay to 0. However, $Pm\bar{3}n$ symmetry cannot allocate 15 × 2 "molecular" hydrogens and 8 × 2 "hydride" ones. Inspection of movies of the trajectories indicate a continuous rearrangement between various pairings of the hydrogens, averaging to cubic symmetry.

It is interesting that Weaire−Phelan Ba_8H_{46} is synthesized at substantially lower pressures than existing superconducting polyhydrides and can be recovered to 20−25 GPa (Figure S11), close to the pressures where barium metal forms complex structures.[52,53] Our DFT calculations find that if the MD pressure is reduced to 0 GPa, significant diffusion occurs and molecular H_2 and BaH_2 form (Figure S12). Thus, it is unlikely that Ba_8H_{46} can be recovered to ambient conditions without further chemical doping.

In summary, using Ba as a host and exploding its ability to act as a template for type-I clathrates, we have identified the formation of hydrogen cages H_{20} and H_{24}. Ba readily interacts with H_2, leading to an unprecedented Ba_8H_{46} at 50 GPa with stability down to 27 GPa, a doubly unique Weaire−Phelan structure. This is the most efficient way of hydrogen packing. Theoretical calculations predict that the cages would hold nonmolecular H_2. The discovery of the formation of highly symmetric hydrogen cages at relatively low pressures broadens the hydrogen-bearing searches for potential low-pressure fundamental research in the superconductivity field. At the modeling level, the cubic structure is not dynamically stable within the harmonic approximation and (classical) molecular dynamics is required to stabilize it close to the experimentally observed cubic phase. We expect that including quantum effects (e.g., via path integral molecular dynamics) would further help stabilize the cubic phase, but these calculations are currently prohibitive. While the Ba polyhydride has strong Jahn−Teller distortions, these are stabilized and symmetrized by nuclear motion at room temperature. This Weaire−Phelan structure which optimizes the metal−atomic hydrogen ratio will be a reference that leads future experimental and theoretical work which could be based on hydrogen packing and clustering instead of increasing the amount of hydrogen per metallic atom. This novel structure type opens up the possibility of superconducting polyhydrides below megabar pressures, a massive step toward ambient-conditions superconductivity.

■ ASSOCIATED CONTENT

Supporting Information

The Supporting Information is available free of charge at https://pubs.acs.org/doi/10.1021/acs.jpclett.1c00826.

The experimental and theoretical methods, electronic and phonon band structures, experimental and calculated unit cell parameters, and H−H distances (PDF)

■ AUTHOR INFORMATION

Corresponding Authors

Miriam Peña-Alvarez − *Centre for Science at Extreme Conditions and School of Physics and Astronomy, University of Edinburgh, Edinburgh EH8 8AQ, U.K.;* orcid.org/0000-0001-7056-7158; Email: mpenaal@ed.ac.uk

Eugene Gregoryanz − *Centre for Science at Extreme Conditions and School of Physics and Astronomy, University of Edinburgh, Edinburgh EH8 8AQ, U.K.; Center for High Pressure Science and Technology Advanced Research, Shanghai 100094, P.R. China; Key Laboratory of Materials Physics, Institute of Solid State Physics, Hefei 230031, P.R. China*; Email: e.gregoryanz@ed.ac.uk

Authors

Jack Binns − *Center for High Pressure Science and Technology Advanced Research, Shanghai 100094, P.R. China;* orcid.org/0000-0001-5421-6841

Miguel Martinez-Canales − *Centre for Science at Extreme Conditions and School of Physics and Astronomy, University of Edinburgh, Edinburgh EH8 8AQ, U.K.*

Bartomeu Monserrat − *Department of Materials Science and Metallurgy, University of Cambridge, Cambridge CB3 0FS, U.K.; Cavendish Laboratory, University of Cambridge, Cambridge CB3 0HE, U.K.;* orcid.org/0000-0002-4233-4071

Graeme J. Ackland − *Centre for Science at Extreme Conditions and School of Physics and Astronomy, University of Edinburgh, Edinburgh EH8 8AQ, U.K.*

Philip Dalladay-Simpson − *Center for High Pressure Science and Technology Advanced Research, Shanghai 100094, P.R. China*

Ross T. Howie − *Center for High Pressure Science and Technology Advanced Research, Shanghai 100094, P.R. China*

Chris J. Pickard − *Department of Materials Science and Metallurgy, University of Cambridge, Cambridge CB3 0FS, U.K.; Advanced Institute for Materials Research, Tohoku University, Sendai 980-8577, Japan;* orcid.org/0000-0002-9684-5432

Complete contact information is available at: https://pubs.acs.org/10.1021/acs.jpclett.1c00826

Notes

The authors declare no competing financial interest.

■ ACKNOWLEDGMENTS

The authors thank Prof. M. McMahon for access to facilities necessary for sample preparation and Liam Kelsall for his

assistance during sample loadings. The authors acknowledge the European Synchrotron Radiation Facility for provision of synchrotron radiation facilities at the ID15B beamline under Proposal HC-3934. The authors also thank the PETRA synchrotron facility at the P02.2 beamline under Proposal I-20190519 EC; GSECARS-(13-IDD) APS under proposals 216253, 208124, and 179388; HPCAT (16-IDD)-APS under proposal 169391; and BL10XU in Spring 8. The research leading to this result has been supported by the project CALIPSOplus under the grant agreement 730872 from the E.U. Framework Programme for Research and Innovation HORIZON 2020. M.P.A., E.G., and G.J.A. would like to acknowledge the financial support of the European Research Council (ERC) grant "Hecate" reference no. 695527 secured by Graeme Ackland. M.P.A. acknowledges the financial support of the UKRI Future leaders fellowship Mrc-Mr/T043733/1. M.M.C., G.J.A., C.J.P., and B.M. acknowledge the EPSRC UKCP project EP/P022561. B.M. acknowledges support from the Gianna Angelopoulos Programme for Science, Technology, and Innovation and from the Winton Programme for the Physics of Sustainability. R.T.H. would like to acknowledge the support of the National Science Foundation of China (Grant No. 11974034).

REFERENCES

(1) Ashcroft, N. W. Hydrogen dominant metallic alloys: high temperature superconductors? *Phys. Rev. Lett.* **2004**, *92*, 187002.
(2) Zurek, E.; Hoffmann, R.; Ashcroft, N.; Oganov, A. R.; Lyakhov, A. O. A little bit of lithium does a lot for hydrogen. *Proc. Natl. Acad. Sci. U. S. A.* **2009**, *106*, 17640−17643.
(3) Wang, H.; Tse, J. S.; Tanaka, K.; Iitaka, T.; Ma, Y. Superconductive sodalite-like clathrate calcium hydride at high pressures. *Proc. Natl. Acad. Sci. U. S. A.* **2012**, *109*, 6463−6466.
(4) Lonie, D. C.; Hooper, J.; Altintas, B.; Zurek, E. Metallization of magnesium polyhydrides under pressure. *Phys. Rev. B: Condens. Matter Mater. Phys.* **2013**, *87*, 054107.
(5) Hooper, J.; Altintas, B.; Shamp, A.; Zurek, E. Polyhydrides of the alkaline earth metals: a look at the extremes under pressure. *J. Phys. Chem. C* **2013**, *117*, 2982−2992.
(6) Hooper, J.; Terpstra, T.; Shamp, A.; Zurek, E. Composition and constitution of compressed strontium polyhydrides. *J. Phys. Chem. C* **2014**, *118*, 6433−6447.
(7) Struzhkin, V. V.; Kim, D. Y.; Stavrou, E.; Muramatsu, T.; Mao, H.-k.; Pickard, C. J.; Needs, R. J.; Prakapenka, V. B.; Goncharov, A. F. Synthesis of sodium polyhydrides at high pressures. *Nat. Commun.* **2016**, *7*, 12267.
(8) Zurek, E. Hydrides of the alkali metals and alkaline earth metals under pressure. *Comments Inorg. Chem.* **2017**, *37*, 78−98.
(9) Mishra, A. K.; Muramatsu, T.; Liu, H.; Geballe, Z. M.; Somayazulu, M.; Ahart, M.; Baldini, M.; Meng, Y.; Zurek, E.; Hemley, R. J. New calcium hydrides with mixed atomic and molecular hydrogen. *J. Phys. Chem. C* **2018**, *122*, 19370−19378.
(10) Drozdov, A.; Kong, P.; Minkov, V.; Besedin, S.; Kuzovnikov, M.; Mozaffari, S.; Balicas, L.; Balakirev, F.; Graf, D.; Prakapenka, V.; et al. Superconductivity at 250 K in lanthanum hydride under high pressures. *Nature* **2019**, *569*, 528−531.
(11) Somayazulu, M.; Ahart, M.; Mishra, A. K.; Geballe, Z. M.; Baldini, M.; Meng, Y.; Struzhkin, V. V.; Hemley, R. J. Evidence for superconductivity above 260 K in lanthanum superhydride at megabar pressures. *Phys. Rev. Lett.* **2019**, *122*, 27001.
(12) Snider, E.; Dasenbrock-Gammon, N.; McBride, R.; Debessai, M.; Vindana, H.; Vencatasamy, K.; Lawler, K. V.; Salamat, A.; Dias, R. P. Room-temperature superconductivity in a carbonaceous sulfur hydride. *Nature* **2020**, *586*, 373−377.
(13) Ma, L.; Wang, K.; Xie, Y.; Yang, X.; Wang, Y.; Zhou, M.; Liu, H.; Liu, G.; Wang, H.; Ma, Y. Experimental observation of superconductivity at 215 K in calcium superhydride under high pressures. *arXiv (Condensed Matter, Superconductivity)*, March 30, 2021, 2103.16282, ver. 1. https://arxiv.org/abs/2103.16282v1.
(14) Li, Z.; He, X.; Zhang, C.; Zhang, S.; Feng, S.; Wang, X.; Yu, R.; Jin, C. Superconductivity above 200 K Observed in Superhydrides of Calcium. *arXiv (Condensed Matter, Superconductivity)*, March 31, 2021, 2103.16917, ver. 1. https://arxiv.org/abs/2103.16917v1.
(15) Li, Y.; Hao, J.; Liu, H.; Tse, J. S.; Wang, Y.; Ma, Y. Pressure-stabilized superconductive yttrium hydrides. *Sci. Rep.* **2015**, *5*, 9948.
(16) Liu, H.; Naumov, I. I.; Hoffmann, R.; Ashcroft, N.; Hemley, R. J. Potential high-Tc superconducting lanthanum and yttrium hydrides at high pressure. *Proc. Natl. Acad. Sci. U. S. A.* **2017**, *114*, 6990−6995.
(17) Peng, F.; Sun, Y.; Pickard, C. J.; Needs, R. J.; Wu, Q.; Ma, Y. Hydrogen clathrate structures in rare earth hydrides at high pressures: possible route to room-temperature superconductivity. *Phys. Rev. Lett.* **2017**, *119*, 107001.
(18) Li, X.; Huang, X.; Duan, D.; Pickard, C. J.; Zhou, D.; Xie, H.; Zhuang, Q.; Huang, Y.; Zhou, Q.; Liu, B.; Cui, T. Polyhydride CeH_9 with an atomic-like hydrogen clathrate structure. *Nat. Commun.* **2019**, *10*, 3461.
(19) Londono, D.; Finney, J. L.; Kuhs, W. F. Formation, stability, and structure of helium hydrate at high pressure. *J. Chem. Phys.* **1992**, *97*, 547−552.
(20) Loveday, J.; Nelmes, R.; Guthrie, M.; Klug, D.; Tse, J. Transition from cage clathrate to filled ice: the structure of methane hydrate III. *Phys. Rev. Lett.* **2001**, *87*, 215501.
(21) Yamanaka, S. Silicon clathrates and carbon analogs: high pressure synthesis, structure, and superconductivity. *Dalton Trans* **2010**, *39*, 1901−1915.
(22) Yamanaka, S.; Enishi, E.; Fukuoka, H.; Yasukawa, M. High-pressure synthesis of a new silicon clathrate superconductor, Ba_8Si_{46}. *Inorg. Chem.* **2000**, *39*, 56−58.
(23) San-Miguel, A.; Toulemonde, P. High-pressure properties of group IV clathrates. *High Pressure Res.* **2005**, *25*, 159−185.
(24) Geballe, Z. M.; Liu, H.; Mishra, A. K.; Ahart, M.; Somayazulu, M.; Meng, Y.; Baldini, M.; Hemley, R. J. Synthesis and stability of lanthanum superhydrides. *Angew. Chem., Int. Ed.* **2018**, *57*, 688−692.
(25) Koshoji, R.; Kawamura, M.; Fukuda, M.; Ozaki, T. Diverse densest binary sphere packings and phase diagram. *Phys. Rev. E: Stat. Phys., Plasmas, Fluids, Relat. Interdiscip. Top.* **2021**, *103*, 023307.
(26) Wu, G.; Huang, X.; Xie, H.; Li, X.; Liu, M.; Liang, Y.; Huang, Y.; Duan, D.; Li, F.; Liu, B.; et al. Unexpected calcium polyhydride CaH_4: A possible route to dissociation of hydrogen molecules. *J. Chem. Phys.* **2019**, *150*, 044507.
(27) Chen, W.; Semenok, D. V.; Kvashnin, A. G.; Huang, X.; Kruglov, I. A.; Galasso, M.; Song, H.; Duan, D.; Goncharov, A. F.; Prakapenka, V. B.; et al. Synthesis of molecular metallic barium superhydride: pseudocubic BaH_{12}. *Nat. Commun.* **2021**, *12*, 273.
(28) Matsuoka, T.; Fujihisa, H.; Ishikawa, T.; Nakagawa, T.; Kuno, K.; Hirao, N.; Ohishi, Y.; Shimizu, K.; Sasaki, S. Beryllium polyhydride $Be_4H_8(H_2)_2$ synthesized at high pressure and temperature. *Phys. Rev. Materials* **2020**, *4*, 125402.
(29) Feng, X.; Zhang, J.; Gao, G.; Liu, H.; Wang, H. Compressed sodalite-like MgH6 as a potential high-temperature superconductor. *RSC Adv.* **2015**, *5*, 59292−59296.
(30) Frank, F. t.; Kasper, J. Complex alloy structures regarded as sphere packings. I. Definitions and basic principles. *Acta Crystallogr.* **1958**, *11*, 184−190.
(31) Howie, R. T.; Guillaume, C. L.; Scheler, T.; Goncharov, A. F.; Gregoryanz, E. Mixed molecular and atomic phase of dense hydrogen. *Phys. Rev. Lett.* **2012**, *108*, 125501.
(32) Peña-Alvarez, M.; Afonina, V.; Dalladay-Simpson, P.; Liu, X.-D.; Howie, R. T.; Cooke, P. I.; Magdau, I. B.; Ackland, G. J.; Gregoryanz, E. Quantitative rotational to librational transition in dense H_2 and D_2. *J. Phys. Chem. Lett.* **2020**, *11*, 6626−6631.
(33) Gregoryanz, E.; Ji, C.; Dalladay-Simpson, P.; Li, B.; Howie, R. T.; Mao, H.-K. Everything you always wanted to know about metallic hydrogen but were afraid to ask. *Matter and Radiation at Extremes* **2020**, *5* (3), 038101.

https://doi.org/10.1021/acs.jpclett.1c00826
J. Phys. Chem. Lett. 2021, 12, 4910−4916

(34) Kinoshita, K.; Nishimura, M.; Akahama, Y.; Kawamura, H. Pressure-induced phase transition of BaH_2: post Ni_2In phase. *Solid State Commun.* **2007**, *141*, 69−72.
(35) Smith, J. S.; Desgreniers, S.; Tse, J. S.; Klug, D. D. High-pressure phase transition observed in barium hydride. *J. Appl. Phys.* **2007**, *102*, 043520.
(36) Tse, J. S.; Song, Z.; Yao, Y.; Smith, J. S.; Desgreniers, S.; Klug, D. D. Structure and electronic properties of BaH_2 at high pressure. *Solid State Commun.* **2009**, *149*, 1944−1946.
(37) The properties and stoichiometry of BaH_x will be discussed in a separate publication.
(38) Fei, Y.; Ricolleau, A.; Frank, M.; Mibe, K.; Shen, G.; Prakapenka, V. Toward an internally consistent pressure scale. *Proc. Natl. Acad. Sci. U. S. A.* **2007**, *104*, 9182−9186.
(39) Altomare, A.; Cuocci, C.; Giacovazzo, C.; Moliterni, A.; Rizzi, R.; Corriero, N.; Falcicchio, A. EXPO2013: a kit of tools for phasing crystal structures from powder data. *J. Appl. Crystallogr.* **2013**, *46*, 1231−1235.
(40) Pickard, C. J.; Needs, R. High-pressure phases of silane. *Phys. Rev. Lett.* **2006**, *97*, 045504.
(41) Pickard, C. J.; Needs, R. Ab initio random structure searching. *J. Phys.: Condens. Matter* **2011**, *23*, 053201.
(42) Clark, S. J.; Segall, M. D.; Pickard, C. J.; Hasnip, P. J.; Probert, M. I.; Refson, K.; Payne, M. C. First principles methods using CASTEP. *Z. Kristallogr. - Cryst. Mater.* **2005**, *220*, 567−570.
(43) Weaire, D.; Phelan, R. A counter-example to Kelvin's conjecture on minimal surfaces. *Philos. Mag. Lett.* **1994**, *69*, 107−110.
(44) Gabbrielli, R.; Meagher, A. J.; Weaire, D.; Brakke, K. A.; Hutzler, S. An experimental realization of the Weaire−Phelan structure in monodisperse liquid foam. *Philos. Mag. Lett.* **2012**, *92*, 1−6.
(45) Kasper, J. S.; Hagenmuller, P.; Pouchard, M.; Cros, C. Clathrate structure of silicon Na8Si46 and NaxSi136 (x 11). *Science* **1965**, *150*, 1713−1714.
(46) Kawaji, H.; Horie, H.-o.; Yamanaka, S.; Ishikawa, M. Superconductivity in the silicon clathrate compound (Na, Ba) x S i 46. *Phys. Rev. Lett.* **1995**, *74*, 1427.
(47) Fukuoka, H.; Kiyoto, J.; Yamanaka, S. Superconductivity of Metal Deficient silicon clathrate compounds, Ba_{8-x} Si_{46} (0.1 x 1.4). *Inorg. Chem.* **2003**, *42*, 2933−2937.
(48) Semenok, D. V.; Zhou, D.; Kvashnin, A. G.; Huang, X.; Galasso, M.; Kruglov, I. A.; Ivanova, A. G.; Gavriliuk, A. G.; Chen, W.; Tkachenko, N. V.; et al. Novel strongly correlated europium superhydrides. *J. Phys. Chem. Lett.* **2021**, *12*, 32−40.
(49) Wang, H.; Tse, J. S.; Tanaka, K.; Iitaka, T.; Ma, Y. Superconductive sodalite-like clathrate calcium hydride at high pressures. *Proc. Natl. Acad. Sci. U. S. A.* **2012**, *109*, 6463−6466.
(50) Errea, I.; Belli, F.; Monacelli, L.; Sanna, A.; Koretsune, T.; Tadano, T.; Bianco, R.; Calandra, M.; Arita, R.; Mauri, F.; et al. Quantum crystal structure in the 250-kelvin superconducting lanthanum hydride. *Nature* **2020**, *578*, 66−69.
(51) Martinez-Canales, M.; Pickard, C. J.; Monserrat, B.; Ackland, G. J. Raw data for Barium Polyhydride, [dataset]. University of Edinburgh. School of Physics & Astronomy. https://doi.org/10.7488/ds/3028. 2021.
(52) Reed, S. K.; Ackland, G. J. Theoretical and computational study of high-pressure structures in barium. *Phys. Rev. Lett.* **2000**, *84*, 5580.
(53) Loa, I.; Nelmes, R.; Lundegaard, L.; McMahon, M. Extraordinarily complex crystal structure with mesoscopic patterning in barium at high pressure. *Nat. Mater.* **2012**, *11*, 627−632.

https://doi.org/10.1021/acs.jpclett.1c00826
J. Phys. Chem. Lett. 2021, 12, 4910−4916